Increased Resting Brain Entropy in Mild to Moderate Depression was Decreased by Nonpharmacological Treatment

Dong-Hui Song[1,2], Yin Wang[1,2*], Ze Wang[3*]

1. State Key Laboratory of Cognitive Neuroscience and Learning, Beijing Normal University, Beijing, China
2. IDG/McGovern Institute for Brain Research, Beijing Normal University, Beijing, China
3. Department of Diagnostic Radiology and Nuclear Medicine, University of Maryland School of Medicine, Baltimore, MD, USA

*** Corresponding author: Yin Wang, Ph.D.**
No.19, Xinjiekouwai St, Haidian District, Beijing, 100875, CN
Email: mirrorneuronwang@gmail.com

*** Corresponding author: Ze Wang, Ph.D.**
670 W Baltimore St, Baltimore, MD, 21201, USA
Email: ze.wang@som.umaryland.edu
Telephone: 410-706-2797

Abstract:

Entropy indicates systematic irregularity and information capacity. Recent years have seen increasing interest in assessing regional brain entropy (BEN) using fMRI in healthy controls (HCs) and patients with various brain diseases. Depression and anti-depressant related BEN alterations have been reported in several initial studies. Re-examining these effects using independent cohort is crucial given the high complexity of depression. In this study, we used open data from OpenNeuro from 46 mild to moderate depression patients and 20 HCs to examine regional BEN and its changes due to nonpharmacological treatment (14 patients underwent nonpharmacological treatment). Functional connectivity (FC) analysis was performed to assess the inter-regional relationship between the brain regions showing BEN effects and the rest of the brain. Compared to HCs, depression patients showed increased BEN in left DLPFC, precuneus, and limbic system, including the amygdala, parahippocampal gyrus and hippocampus. Increased BEN in DLPFC, precuneus, and amygdala were suppressed by a nonpharmacological treatment in each individual patient. HCs had positive FC between left and right DLPFC and negative FC between left DLPFC and limbic areas, while patients had abnormally lower or negative FC between left and right DLPFC and positive FC between left DLPFC and the limbic area. These left DLPFC seeded FC changes in patients were reverted after nonpharmacological treatment. The findings highlight the left DLPFC and limbic system in depression and the treatment effects, and patients with depression exhibit significant emotion dysregulation, which is effectively addressed by nonpharmacological treatment targeting the top-down emotion regulation functions mediated by the DLPFC-limbic system. Different from existing literature, these results suggest the entropy/irregularity of DLPFC and limbic system as a potential mechanism underlying depression and suggest BEN in left DLPFC as a potential personalized marker for assessing depression and the corresponding nonpharmacological treatment effects.

Keywords

Brain entropy, Depression, Nonpharmacological treatment, Resting state fMRI

1. Introduction

Entropy refers to the irregularities and disturbances of the dynamic system (Clausius 1862). The second law of thermodynamics states that entropy increases over time, eventually reaching a state of maximum chaos and disorder in an isolated system. In information theory, entropy quantifies uncertainty, surprise, and the amount of information (Shannon 1948). A living system is a highly self-organizing system that constantly interacts with the external environment to reduce its own entropy to maintain proper functioning (Odum 1988, Sneyd, Theraula et al. 2001). The human brain, one of the most complex systems in the world, consumes a disproportional amount of body energy even without performing any overt tasks (Magistretti and Allaman 2015), which has been postulated to maintain the brain's normal functional state (Friston, Kilner et al. 2006, De Ridder, Vanneste et al. 2014) and probably maintain the balance of brain entropy (BEN) (Wang 2021). Nevertheless, BEN can serve as a metric to depict the complex dynamic state of the brain associated with normal and disordered brain function.

In the human brain, regional BEN has been increasingly assessed using resting state fMRI (rsfMRI) , providing diverse information such as regional perfusion and the amplitude of low-frequency fluctuations (Song, Da Chang et al. 2018, Song, Chang et al. 2019). Using rsfMRI from a large cohort of healthy subjects, we previously identified normal BEN distributions at rest (Wang, Li et al. 2014) and their associations with age, sex, education, and neurocognition (Wang 2021), even after controlling for motion and physiological variables (Del Mauro and Wang 2023). The neurocognitive correlates of resting BEN were further indicated by the correlations between regional BEN and the magnitude of task activations and task de-activations in the corresponding activated and de-activated brain regions (Lin, Chang et al. 2022) as well as the various functional task-induced BEN changes (Camargo, Del Mauro et al. 2024). The clinical and translational research suggests that BEN alterations are associated with various brain diseases (Sokunbi, Fung et al. 2013, Zhou, Xu et al. 2014, Li, Fang et al. 2016, Zhou, Zhuang et al. 2016, Xue, Yu et al. 2019, Liu, Song et al. 2020, Wang

and Initiative 2020, Kuang, Gao et al. 2021, Ji, Zhang et al. 2022, Fu, Liang et al. 2023, Jiang, Cai et al. 2023), including major depressive disorder (MDD) (Lin, Lee et al. 2019, Liu, Song et al. 2019, Liu, Song et al. 2020). Importantly, we have shown that regional BEN can be modulated by repetitive transcranial magnetic stimulations (rTMS) (Chang, Song et al. 2018, Song, Chang et al. 2019), caffeine (Chang, Song et al. 2018), and medication (Liu, Song et al. 2019, Liu, Song et al. 2020).

Depression is a common mental disorder characterized by persistent sadness and lack of interest or pleasure in previously rewarding or enjoyable activities (https://www.who.int/news-room/fact-sheets/detail/depression). Despite numerous research efforts, the brain mechanisms of this extremely inhomogeneous disease remain unclear (Chaudhury, Liu et al. 2015). By characterizing the temporal dynamics of the brain, BEN could open a unique window to advance our understanding of the regional neural mechanisms of depression, offering an opportunity to pinpoint region-specific targets for future intervention studies. Our recent research suggests that, in comparison to the healthy controls (HCs), the MDD group has reduced BEN in the medial orbitofrontal cortex (MOFC)/subgenual cingulate cortex (sgACC), which is a component of the default mode network (DMN) and increased BEN in the motor cortex (MC). Interestingly, lower BEN in MOFC/sgACC was associated with lower levels of depression, while higher BEN in MC was associated with lower disease severity (Liu, Song et al. 2019, Liu, Song et al. 2020). The seemingly contradictory results between the cross-sectional comparisons and the within-subject correlations were also reported by Fu et al. (Fu, Liang et al. 2023) who observed reduced BEN in the right lateral orbitofrontal cortex (LOFC), but found that higher BEN therein was related to higher disease severity in MDD patients. In another entropy study (Lin, Lee et al. 2019), Lin et al. reported higher BEN in the left frontoparietal network (FPN) in late-life depressed older adults compared to HCs, which was related to lower geriatric depression scale scores (Lin, Lee et al. 2019). While these studies clearly demonstrated the potential of BEN for identifying regional changes and their associations with depression, the cross-sectional differences in BEN were all opposite to the within-patient BEN-disease correlation results. The within-patient BEN-disease correlation results also showed discrepancy between studies. These inconsistencies could be caused by various factors

common in MDD research, including use of different antidepressants, medication history, recurrence, disease status during MRI scanning, and heterogeneity between individuals, which have been reported and discussed in other studies (Yan, Chen et al. 2019, Schmaal, Pozzi et al. 2020, Klooster and Siddiqi 2023).

To avoid these often difficult-to-control confounds, we aim to focus on BEN in patients with mild to moderate depression, which can effectively avoid the influence of medication and medication history. Using a mild to moderate depression cohort may help provide clues to the early onset and progression of depression as an affective/mood spectrum (Hudson, Mangweth et al. 2003). We also aimed to answer a clinically important question of whether BEN can track treatment effects through nonpharmacological treatment, as we previously demonstrated that BEN can monitor the effectiveness of drug treatment in MDD (Liu, Song et al. 2019, Liu, Song et al. 2020). Based on previous studies (Lin, Lee et al. 2019, Liu, Song et al. 2019, Liu, Song et al. 2020), we assume that brain regions affected by depression predominantly involve the DMN, FPN and sensorimotor network (SMN). We expect a decrease in BEN within these regions following nonpharmacological treatment in individuals with depression. These hypotheses are supported by insights gained from BEN into the neural mechanisms of healthy adults. Recently, we utilized multiple MRI scanners to confirm replicable increased BEN in the DMN including the posterior cingulate cortex (PCC), precuneus (PCu), and angular gyrus (AG) during rumination (Song, et al. 2023), which is closely related to depression and is considered a common mechanism linking depressive risk factors to depression (Spasojević and Alloy 2001, Whisman, du Pont et al. 2020). Furthermore, high frequency rTMS of the left dorsolateral prefrontal cortex (DLPFC), the FDA-approved therapy for MDD, has been observed to reduce BEN in the MOFC/sgACC (Donghui Song, Zhang et al. 2017, Song, Chang et al. 2019) and using a new coherence measurement method, temporal coherence mapping (TCM) (Wang 2021), we also recently found increased coherence in the AG (Song, et al.2023). These studies suggest that depression may be associated with increased BEN of DMN and FPN; BEN in mild to moderate depression will be decreased by nonpharmacological treatment.

2. Methods

2.1 Dataset

2.1.1 Participants

We identified two datasets from OpenNeuro: ds002748 and ds003007 which were released by Bezmaternykh et al (https://openneuro.org/datasets/ds002748 and https://openneuro.org/datasets/ds003007). Fifty-one participants with mild and moderate depression participants DEP and 21 HCs were included. 14 depression patients (Treat) received nonpharmacological treatment (8 patients received brief cognitive behavioral therapy, 6 patients underwent a real-time fMRI neurofeedback course) and were scanned before (Treat Pre) and after treatment (Treat Post).

2.1.2. Clinical Measures

Zung Self Rating Depression Scale (SDS) (Zung 1965) and Beck Depression Inventory (BDI) (Beck, Steer et al. 1987) were used to assess depression severity. Additionally, the Rumination Response Scale (RRS) (Spasojević and Alloy 2001) was used to assess the degree of rumination in the DEP group and the Treat group.

2.1.3. Treatments

Cognitive-behavioral therapy (CBT): each participant received 8 common and 8 personalized treatment sessions. Five patients were included in the common treatment sessions led by a psychiatrist and a clinical psychologist at a time. Each common session contained a course describing automatic thought, the connection between automatic thought and emotions, cognitive biases, thoughts modification techniques, positive reappraisal, and assertiveness. Personalized treatment sessions involved personalized and symptom-focused intervention, problems detection, work with priorities, belief-emotion connections, automatic thoughts, and cognitive biases detection and modification.

Neurofeedback (NFB): Total scanning time was approximately 30 minutes for each session. Five minutes were spent on the placement of participant into scanner and acquisition of reference images, and 25 minutes were dedicated to neurofeedback per session. In even sessions, participants spent 10 minutes of neurofeedback time on a transfer run in which they received no feedback and had to rely on their established strategies of signal regulation. In total, each participant received 8 individual sessions.

2.1.4. fMRI Acquisition

MRI images were acquired in the International Tomography Center, Novosibirsk, using a 3□T Ingenia scanner (Philips Inc). Anatomical images were acquired with a T1-weighted 3D turbo field echo sequence with a voxel size of 1x1x1 mm^3. fMRI images were acquired using a T2*-weighted echo planar imaging sequence. Acquisition parameters were: voxel size=2x2x5 mm^3, repetition time=2.5 s, echo time=35 ms. Participants were asked to lie still with eyes closed during the scan. 100 volumes were required. More details about these data can be found in (Bezmaternykh, Melnikov et al. 2021).

2.2 MRI preprocessing

MRI images were preprocessed using custom scripts based on FSL (version=6.06.5) (Sm ith, Jenkinson et al. 2004),Nilearn (version=0.10.2) (https://nilearn.github.io/stable/index.htm l) and Nipype (Gorgolewski, Burns et al. 2011). First, the structural images were segmented i nto gray matter (GM), white matter (WM), and cerebrospinal fluid (CSF) using FAST (Zhan g, Brady et al. 2001), and then normalized to MNI152 space using FLIRT (Jenkinson and Smi th 2001, Jenkinson, Bannister et al. 2002, Greve and Fischl 2009). The functional images und erwent preprocessing through the following steps:

1. The first two time points were discarded to remove signal from the non-steady state.
2. Slice timing was corrected for the remaining time points.
3. Head motion correction was performed using MCFLIRT (Jenkinson, Bannister et al. 2002), generating motion parameter files and an average functional image.

4. FLIRT was used to register the segmented structural image to the average functional image to extract signal of WM and CSF.

5. The average signals of WM and CSF were extracted from the functional image according to segmented structural brain.

6. Framewise displacement (FD) (Power, Barnes et al. 2012) was computed based motion parameter, and the mean FD was calculated using Nipype.

7. Detrending and temporal bandpass filtering (0.01–0.1 Hz) was performed. Nuisance components were regressing out including the six motion parameters, as well as the average WM signals and average CSF signals.

8. Functional images were smoothed with a 6 mm full width at half maximum (FWHM) Gaussian kernel.

2.3 BEN mapping calculation

The BEN mapping toolbox (BENtbx) (Wang, Li et al. 2014) was used to calculate BEN at each voxel of the preprocessed rsfMRI data using sample entropy (SampEn) (Richman and Moorman 2000). The toolbox can be found at https://www.cfn.upenn.edu/zewang/BENtbx.php and https://github.com/zewangnew/BENtbx. More details of BEN calculation can be found in the original BENtbx paper (Wang et al., 2014) or our previous studies (Song, Chang et al. 2019, Liu, Song et al. 2020, Wang and Initiative 2020, Wang 2021, Lin, Chang et al. 2022). In this study, the window length was set to 3 and the cut off threshold was set to 0.6 based on optimized parameters (Wang, Li et al. 2014). BEN maps were then normalized to MNI space for group analysis. To reduce variability due to noise, BEN maps were smoothed with an isotropic Gaussian kernel (FWHM = 8 mm).

2.4 Functional connectivity analysis

In addition to regional BEN effects, we are also interested in the relationship between the identified regions and the rest of the brain. To this end, we performed functional connectivity (FC) analysis to assess whole-brain connectivity of the region where significant changes in BEN were observed in both cross-sectional (Treat Pre vs HCs) and longitudinal

analyses (Treat Post- Treat Pre). In other words, we used the region showing the maximum BEN difference from longitudinal analyses as the seed of the FC analysis. Through this seed-based FC analysis, we aimed to find alterations of the network connected to the BEN altered region in DEP, complementing the region-independent BEN alteration analysis.

The specific seed-based FC calculation was as follows: FC maps were calculated by custom python scripts based on Nilearn (https://nilearn.github.io/stable/index.html). Preprocessed fMRI images were normalized to MNI space. A 3mm-radius spherical region of interest (ROI) centered at the peak MNI coordinate (-18, 18, 54) (left DLPFC) of BEN differences between pre and post treatment as seed, then mean rsfMRI time series was extracted from the seed and correlated to time series of all voxels in whole brain. The correlation coefficient was measured as the amplitude of FC and Fisher z-transformed to improve the normality before performing group level analysis.

3 Statistical analysis

All statistical analyses were conducted using custom python scripts.

3.1 Demographic information and clinical measures analysis

Two-sample t-tests were employed to assess differences in age, Raven scores, and clinic al measures across different groups, while paired t-tests were utilized to assess changes befor e and after treatment. Chi-square tests were conducted to examine sex differences between th e different groups.

3.2 Cross-sectional BEN differences between DEP, Treat, and HCs

Two-sample t-tests were utilized to examine baseline BEN differences between the DEP, Treat and HCs groups. Sex, age, and mean FD were included as covariates.

3.3 Neurosynth Decoding

To mitigate the potential statistical bias due to the small sample size, we meta-

analytically decoded the functional terms associated with the unthresholded t-maps of the several BEN comparisons (between the DEP, Treat Pre, and the HCs group). Neurosynth (https://neurosynth.org) is a meta-analytic tool that contains 14371 functional neuroimage studies with meta-analyses of 1334 terms (Yarkoni, Poldrack et al. 2011). The analysis method can be found in (https://neurosynth.org/analyses/terms/). We first uploaded unthresholded t-maps to NeuroVault (Gorgolewski, Varoquaux et al. 2015) and then used the Neurosynth decoder function provided by NeuroVault to compute a voxel-wise Pearson correlation coefficient between the t-value and each of the term-based z-statistic maps extracted from Neurosynth. Out of the 1,334 terms, the first 100 terms are initially selected based on positive or negative correlation strength, after all anatomical, redundant, and methodologic terms were excluded, then top 30 terms were visualized as word clouds. Unthresholded t-statistical maps archived in NeuroVault (https://neurovault.org/collections/YSQTCFYO/) and can be used to generate the complete list of terms.

3.3 Treatment effects on BEN

Treatment effects of BEN were assessed using paired-t test (Treat Post – Treat Pre). Mean FD was included as covariate.

3.4 Correlations of BEN to Clinical Measures

Utilizing the suprathreshold clusters as regions-of-interest (ROIs) derived from cross-sectional analyses (DEP vs HCs, Treat Pre vs HCs) and longitudinal analysis (Treat Post - Treat Pre), we extracted the mean BEN values from multiple ROIs and employed multiple regression to examine the correlation between clinical measures (SDS, BDI and RRS) and mean BEN values within the ROIs, separately in the DEP group and the Treat Pre group. Age, sex, and mean FD were included as covariates.

3.5 FC Analysis

FC underwent a similar analysis as BEN, which included examining FC differences between the DEP and HCs groups, assessing treatment effects on FC in the Treat group, and examining correlations between FC and clinical measures.

4 Results

4.1. Demographic information and Quality Control

Five depression patients were excluded from the DEP group, including one with excessive head motion (mean FD > 0.2 mm), one without diagnostic information, one with dysthymia (F34.1), one recurrent depression (F34.9), one with image artifact and one healthy participant was excluded whose Raven scores <70. Ultimately, 46 in DEP group, 20 in HCs group and 14 in Treat group. Table 1 shows specific details about demographic information of participants.

Table 1. Demographic information of participants

Variables	DEP	Treat	HCs	*P1*	*P2*
Age (M±SD)	32.57±8.94	30.43±8.32	32.90±7.40	0.885	0.384
Sex (f/m)	36/10	10/4	14/6	0.472	0.928
Raven (M±SD)	103.39±14.71	104.69±12.17	108.00±13.67	0.265	0.506

Note: M±SD: Mean ± Standard Deviation, f/m: female/male, Raven: Raven Scores, *P1*: Compare between DEP group (n=46) and HCs group (n=20); *P2*: Compare between Treat (n=14) and HCs group (n=20).

4.2. Clinical Measures

Significant differences were observed in SDS, BDI, and RRS scores between the DEP group (including all patients) and the HCs group and between patients in the Treat group and the HCs group. Moreover, there were significant changes in BDI scores detected before and

after treatment (Table 2).

Table 2. Clinical measures differences from different groups

Variables	DEP (M±SD)	Treat Pre (M±SD)	Treat Post (M±SD)	HCs (M±SD)	*P1*	*P2*	*P3*	*P4*
SDS	47.10±6.96	50.46±5.53	46.45±7.49	33.06±5.70	<0.001	<0.001	<0.001	0.096
BDI	21.62±10.01	25.79±9.78	15.82±9.97	4.35±4.60	<0.001	<0.001	<0.001	0.021
RRS	55.88±11.39	60.62±7.20	59.18±6.64	40.00±9.76	<0.001	<0.001	<0.001	0.479

Note: M±SD: Mean ± Standard Deviation, SDS: Zung Self Rating Depression Scale, BDI: Beck Depression Inventory, RRS: Rumination Response Scale, *P1*: Compare between DEP group (n=40) and HCs group (n=20); *P2*: Compare between Treat Pre (n=13) and HCs group (n=20), *P3*: Compare between Treat Post and HCs group, *P4*: Compare between Treat Pre and Treat Post group (n=11).

4.2 Cross-sectional baseline BEN difference and treatment-induced BEN changes

Compared to the HCs group, DEP (the entire depression group) showed higher BEN in the right parahippocampal gyrus (PHPC), right hippocampus (HPC), right left amygdala (AMY), left putamen, and right posterior medial temporal lobe (pMTG) (Fig 1a, FDR corrected $p< 0.05$). Similarly, patients enrolled in the treatment group (Treat group) exhibited higher BEN in the left DLPFC, right inferior temporal gyrus (ITG), and right putamen compared to the HCs group (Fig. 1 b, FDR corrected $p< 0.05$). While differences in brain regions with higher BEN were found in various group comparisons, the primary source of variation originated from the thresholding approach. HCs vs DEP BEN difference patterns became more consistent when a less stringent statistical threshold (uncorrected voxel-level $p < 0.01$) was used (see S2 Fig.S1). Functional decoding from a large-scale meta-analysis database (Neurosynth) for unthresholded two-sample t-test statistical maps, provided relatively consistent results for both the DEP group and Treat group compared to HCs group. The results suggested positive association with emotion-related functional terms such as "face

expression," "emotional," etc., and negative association with reward-related functional terms, such as "reward," "monetary," etc (Fig1 a, b, all terms are available in S1). Another notable difference lies in the variations in depression severity between the DEP and Treat groups. The overall depression level in the DEP group appears to be milder compared to that in the Treat group (Table 2), particularly when excluding participants in the Treat group from the DEP group (S2 Table S1). Exploratory analysis revealed a distinctive pattern in BEN levels between the Non-Treat group, characterized by milder depression, and the Treat group, characterized by more severe depression. Specifically, higher BEN values were observed in the right DLPFC of individuals in the Non-Treat group, whereas the Treat group exhibited elevated BEN in the left DLPFC (uncorrected voxel-level $p<0.001$, cluster size > 270 mm^3 results are presented in S2 Fig.S2).

For the Treat group, BEN decreased in the left DLPFC, right PHPC, right HPC, right lateral habenula (LHb), right paracentral lobule (PCL), right PCu, right frontal eye fields (FEF), left inferior frontal gyrus (IFG), left primary sensory cortex (PSC), right ITG, right supramarginal gyrus (SMG), right inferior parietal lobe (IPL), right primary motor cortex (PMC), left LOFC, and increased in the right posterior superior temporal sulcus (pSTS), left PSC, left LOFC, left anterior MTG (aMTG) after treatment (Fig.1 c). Mean BEN values were then extracted from the left DLPFC (peak MNI coordinates = (-18, 18, 54)) in the DEP group, Treat group and HCs group. Differences in mean BEN values were tested, revealing that the Treat Pre group had the highest mean BEN values, followed by the DEP group, and the HCs group had the lowest mean values in the left DLPFC (Fig.1 d). At the individual level, mean BEN values in the left DLPFC for participants in the Treat groups decreased compared to before treatment (Fig. 1 d).

Table 3 provides information on clusters exceeding the threshold (FDR corrected $p < 0.05$, cluster size ≥ 81 mm^3), including peak MNI coordinates, cluster size, label on the AAL atlas, and brain regions for BEN analysis.

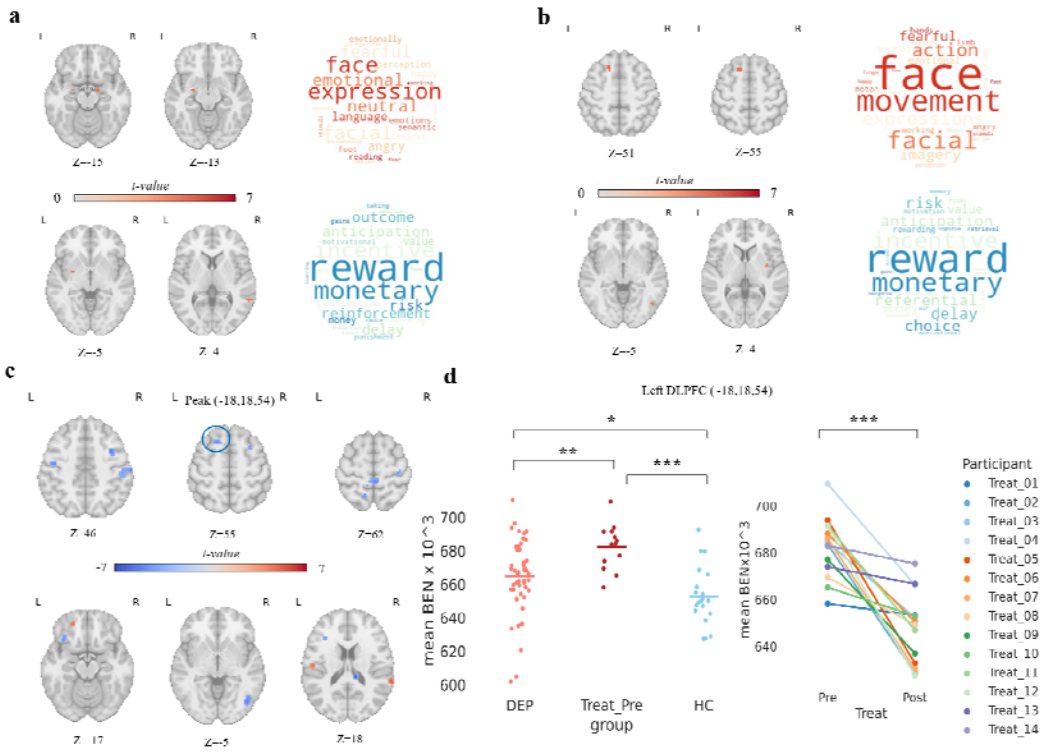

Fig1. DEP vs HCs baseline BEN difference and treatment-induced longitudinal (post - pre) BEN difference. a) left: BEN differences between the entire DEP cohort (n=46) and HCs (n=20). Hot color means higher BEN in DEP; right: Neurosynth decoding for the unthresholded t map of the DEP vs HCs comparison; b) left: differences of baseline BEN of the treatment patient subgroup (Treat Pre) and HCs. Hot color indicates higher BEN in patients; right: Neurosynth decoding for the unthresholded t map of the comparison on the left. Red words describe the positively correlated terms. Blue words describe the negatively correlated terms. The font size is linearly related to the correlation coefficient; c) treatment induced BEN changes (hot color means increased BEN after treatment, cool color means decreased BEN after treatment); d) left: mean baseline BEN values of the suprathreshold cluster (the blue circle in c1) from the entire patient group, treatment group, and HCs. The y-axis represents the mean BEN values × $10^{\wedge 3}$ within the cluster, while the x-axis corresponds to different groups, the horizontal line represents the mean BEN value for the group; right: mean BEN of the prefrontal cortex cluster (blue circle in c) before and after treatment for the treatment cohort. The y-axis represents the mean BEN values × $10^{\wedge 3}$ within the cluster, while the x-axis corresponds to the different treatment stages. For a, b, and c, the significance level was defined by an FDR corrected p< 0.05. The number under each slice indicates its location along the z-axis in the MNI space, and L means left hemisphere, R means right hemisphere, * p<0.05, ** p<0.01, *** p<0.001.

Table 3. Clusters size table for BEN analysis

Contrast	Cluster ID	Peak MNI Coordinate (X, Y, Z)	Peak T Value	Cluster Size (mm^3)	AAL Label	Brain Region
DEP vs HCs	1	(18, -6, -18)	5.106	891	ParaHippocampal_R	PHPC/HPC_R
	1a	(18, -6, -27)	4.919		ParaHippocampal_R	PHPC_R
	2	(-30, -3, -6)	4.736	243	Putamen_L	Putamen_L
	2a	(-24, -6, -12)	4.650		Amygdala_L	AMY_L
	3	(60, -48,3)	4.457	189	Temporal_Mid_R	pMTG_R
Treat Pre vs HCs	1	(-18,21,54)	5.030	378	Frontal_Sup_L	DLPFC_L
	2	(48, -69, -3)	4.764	135	Temporal_inf_R	ITG_R
	3	(36, -3,3)	4.654	81	Putamen_R	Putamen_R
Treat Post vs Treat Pre	1	(12, -9, -27)	-7.902	594	No Label	PHPC_R
	2	(12, -33,18)	-7.003	891	No Label	LHb/HPC_R
	2a	(15, -36,9)	-4.914		No Label	LHb_R
	3	(9, -36,57)	-6.632	1107	Paracentral_Lobule_R	PCL/PCu_R
	4	(39,3,39)	-6.189	1404	Precentral_R	FEF_R
	4a	(27,12,54)	-4.363		Frontal_Mid_R	FEF_R
	5	(-39,24,15)	-5.411	648	Frontal_Inf_Tri_L	IFG_L
	5a	(-48,30,15)	-4.164		Frontal_Inf_Tri_L	IFG_L
	6	(-45, -12,42)	-5.345	756	Postcentral_L	PSC_L
	7	(45, -72, -6)	-5.301	1215	Temporal_Inf_R	ITG_R
	8	(63, -21,45)	-5.229	1512	SupraMarginal_R	SMG_R
	8a	(54, -30,51)	-4.496		Parieral_Inf_R	IPL_R
	9	(-12, -48,69)	-4.990	972	Precuneus_L	PCu_L
	9a	(-12, -57,63)	-4.558		Precuneus_L	PCu_L
	10	(-18,18,54)	-4.925	486	Frontal_Sup_L	DLPFC_L
	11	(-33,27, -21)	-4.784	459	Frontal_Inf_Orb_L	LOFC_L
	12	(33, -24,60)	-4.755	297	Precentral_R	PMC_R
	13	(66, -39,18)	5.432	405	Temporal_Sup_R	pSTS_R
	14	(-54, -15,15)	5.372	702	Postcentral_L	PSC_L
	15	(-21,48, -15)	5.232	513	Frontal_Mid_Orb_L	LOFC_L
	16	(-57,0, -30)	4.192	405	Temporal_Mid_L	aMTG_L

Note: PHPC/HPC: parahippocampal gyrus/hippocampus, AMY: amygdala, pMTG: posterior middle temporal gyrus, DLPFC: dorsolateral prefrontal cortex, ITG: inferior temporal gyrus, HPC: hippocampus, LHb: lateral habenula, PCL: paracentral lobule, PCu: precuneus, FEF: frontal eye fields, IFG: inferior frontal gyrus, PSC: primary sensory cortex, SMG: supramarginal gyrus, IPL: inferior parietal lobe, LOFC: lateral orbitofrontal cortex, PMC: primary motor cortex, pSTS: posterior superior temporal sulcus, aMTG: anterior middle temporal gyrus. L: left, R: right.

Except for the significantly consistent region of left DLPFC from FDR-corrected results from cross-sectional and longitudinal studies, we also extracted mean BEN values from AMY (peak MNI coordinates = (-24, -6, -12)), PHPC/HPC (peak MNI coordinates = (18, -6, -18)) and PCu (peak MNI coordinates = (-12, 48, 69)) in the DEP group, Treat group and HCs group. Differences in mean BEN values were tested, revealing that the Treat Pre group and the DEP group both had higher mean BEN values than the HCs group in the AMY,

PHPC/HPC and PCu, while the mean BEN values were decreased in AMY, PHPC/HPC and PCu after treatment in Treat groups (Fig 2).

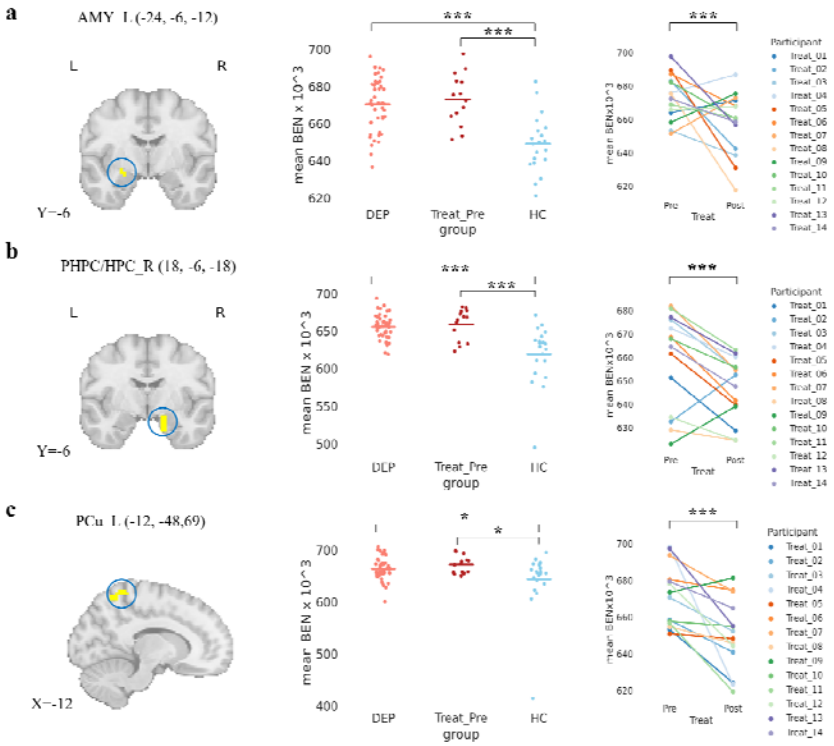

Fig 2. Cross-sectional BEN difference (HCs vs DEP) and treatment-induced longitudinal (post - pre) mean BEN difference in AMY, PHPC/HPC and PCu. a) left: mean baseline BEN values of in AMY (peak MNI coordinates = (-24, -6, 12), blue circle in b) from the entire patient group, treatment group, and HCs. The y-axis represents the mean BEN values × $10^{\wedge 3}$ within the cluster, while the x-axis corresponds to different groups, the horizontal line represents the mean BEN value for the group; right: mean BEN values of AMY before and after treatment for the treatment cohort. The y-axis represents the mean BEN values × $10^{\wedge 3}$ within the cluster, while the x-axis corresponds to the different treatment stages. b) left: mean baseline BEN values of in PHPC/HPC (peak MNI coordinates= (18, -6, -18), blue circle in a) from the entire patient group, treatment group, and HCs. The y-axis represents the mean BEN values × $10^{\wedge 3}$ within the cluster, while the x-axis corresponds to different groups, the horizontal line represents the mean BEN value for the group; right: mean BEN of PHPC/HPC before and after treatment for the treatment cohort. The y-axis represents the mean BEN values × $10^{\wedge 3}$ within the cluster, while the x-axis corresponds to the different treatment stages. c) left: mean baseline BEN values of in PCu (peak MNI coordinates = (-12, -48, 69), blue circle in c) from the entire patient group, treatment group, and HCs. The y-axis represents the mean BEN values × $10^{\wedge 3}$ within the cluster, while the x-axis corresponds to different groups, the horizontal line represents the mean BEN value for the group; right: mean BEN values in PCu before and after treatment for the treatment cohort. The y-axis represents the mean BEN values × $10^{\wedge 3}$ within the cluster, while the x-axis corresponds to the different treatment stages. * p<0.05, ** p<0.01, *** p<0.001.

Correlation analysis indicated that higher BEN in PHPC/HPC in Treat Pre group was correlated with higher SDS scores (Table 4).

Table 4. Correlations of BEN to clinical measures

Brain region	Peak MNI Coordinate (X, Y, Z)	SDS		BDI		RRS	
		DEP	Treat Pre	DEP	Treat Pre	DEP	Treat Pre
DLPFC_L	(-18, -18, 54)	0.283	-0.247	0.123	-0.341	0.301	-0.329
AMY_L	(-24, -6, -12)	-0.137	-0.016	-0.002	0.011	-0.301	-0.273
PHPC/HPC_R	(18, -6, -18)	0.228	0.570*	-0.035	0.413	0.178	0.056
PCu_L	(-12, -48,69)	0.013	0.172	-0.066	0.45	0.218	0.293

Note: SDS: Zung Self Rating Depression Scale, BDI: Beck Depression Inventory, RRS: Rumination Response Scale. DLPFC: dorsolateral prefrontal cortex, AMY: amygdala, PHPC/HPC: parahippocampal gyrus/hippocampus, PCu: precuneus. L: left hemisphere, R: right hemisphere. * $p<0.05$.

4.3 Cross-sectional baseline FC difference and treatment-induced FC changes

The results of whole-brain FC analysis using left DLPFC as seed showed increased FC between left DLPFC and left PHPC/AMY in the DEP group (Fig 3a, voxel-level $p< 0.001$ and cluster size $\geq$135 mm^3) and Tret Pre group (Fig 3b, voxel-level $p< 0.001$ and cluster size $\geq$135 mm^3). Longitudinal analyses showed increased FC in the right DLPFC (Fig 3c, FDR corrected $p<0.05$, cluster size $\geq$270 mm^3). Subsequently, mean FC values were extracted from the right DLPFC (peak MNI coordinates = (36, 51, 27)) in the DEP group, HCs group, and Treat group. Differences in mean FC values were tested, revealing that the Treat Pre group exhibited lower mean left DLPFC-right DLPFC FC values than the DEP group and HCs group (Fig 3d). At the individual level, mean FC values in the right DLPFC for participants in the Treat groups increased compared to before treatment (Fig 3d).

Table 5 provides information on clusters exceeding the threshold (voxel-level $p< 0.001$ and cluster size $\geq$135 mm^3 for cross-sectional analyses, FDR corrected $p<0.05$, cluster size $\geq$270 mm^3 for longitudinal analyses), including peak MNI coordinates, cluster size, labels in the AAL atlas, and brain regions for FC analysis.

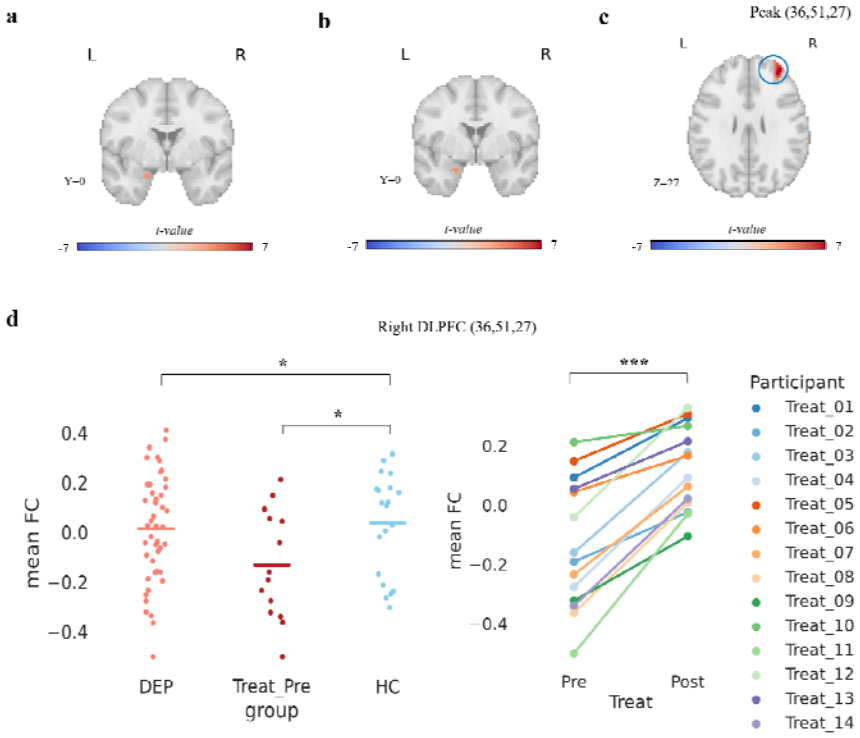

Fig 3. Cross-sectional baseline FC DEP vs HCs difference and longitudinal (post-pre) FC difference. a) FC differences between the entire DEP cohort (n=46) and HCs (n=20). Hot color means higher FC in DEP; b) differences of baseline FC of the treatment patient subgroup and HCs. Hot color means higher BEN in patients; c) treatment induced FC changes (hot color means increased FC after treatment); d) left: mean FC values were extracted from a the right DLPFC cluster from c) (labeled by the blue circle, peak MNI coordinates=(36, 51, 27)), then mean FC values differences were tested for DEP group, Treat Pre group and HCs group, the y-axis represents the mean FC values within the cluster, while the x-axis corresponds to different groups, the horizontal line represents the mean FC value for the group; right: individual-level changes in mean FC values within the specified cluster circled in blue (peak MNI coordinates= (36, 51, 27)) were assessed after treatment and visualized using a line graph. The y-axis represents the mean FC values within the cluster, while the x-axis corresponds to the different treatment stages (Treat Pre and Treat Post). For a and b, the significance level was defined by $p< 0.001$ and cluster size $\geq$135 mm^3, for c, significance level was defined by an FDR corrected $p< 0.05$ and cluster size $\geq$135 mm^3. The number under each slice indicates its location along the y-axis or z-axis in MNI space, and L means left hemisphere, R means right hemisphere. * p<0.05, ***p<0.001.

Table 5. Clusters size tables for FC analysis

Contrast	Cluster ID	Peak MNI Coordinate (X, Y, Z)	Peak Value (t)	Cluster Size (mm^3)	AAL Label	Brain Region

DEP vs HCs	1	(-18,0, -24)	3.722	405	ParaHippocampal_L	PHPC/AMY_L
Treat Pre vs HCs	1	(-21,0, -24)	4.031	162	Amygdala_L	AMY_L
Treat Post-Treat Pre	1	(36, 51, 27)	7.389	1998	Frontal_Mid_R	DLPFC_R

Note: PHPC: parahippocampal gyrus, AMY: amygdala, DLPFC: dorsolateral prefrontal cortex. L: left hemisphere, R: right hemisphere.

Mean left DLPFC FC values also extracted from AMY and HPC in the DEP group, Treat group and HCs group, AMY and HPC are derived from the intersection of results with voxel-level $p< 0.05$ and cluster size ≥ 270 mm^3 from both cross-sectional and longitudinal results of FC. The results indicate that higher left DLPFC-AMY and left DLPFC-HPC FC in DEP group and Treat group than HCs group, then left DLPFC-AMY FC decreased after treatment, and left DLPFC-HPC FC trend to decrease after treatment (marginally significant, p=0.055) (Fig 4).

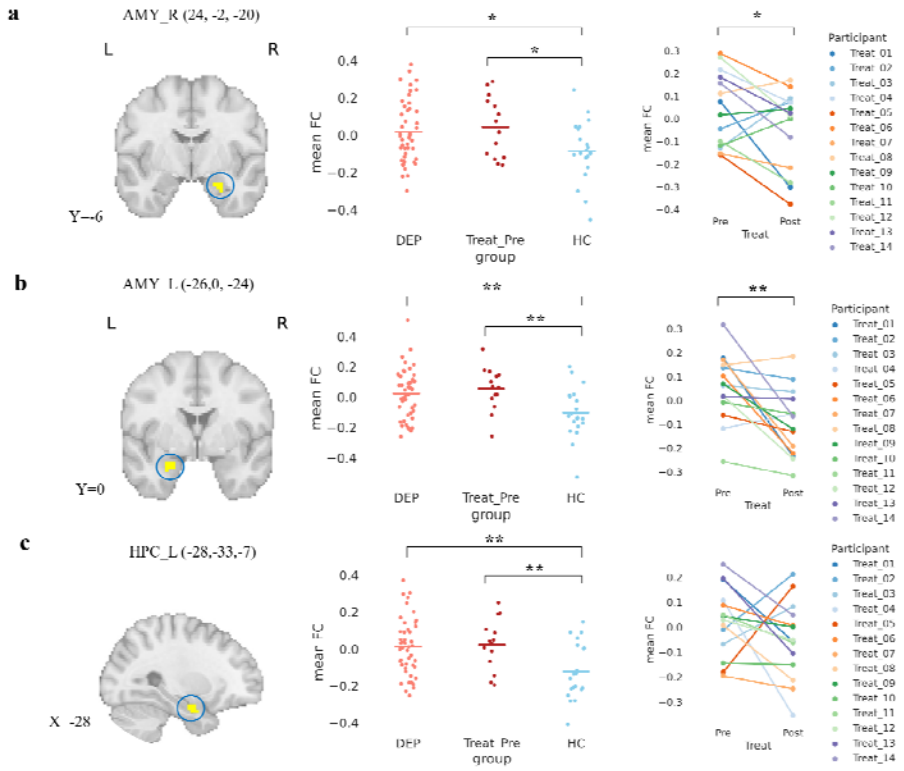

Fig 4. Cross-sectional baseline FC difference between DEP and HCs and longitudinal (post-pre) mean FC values difference in AMY/HPC_R, AMY/HPC_L and HPC_L. a) left: mean baseline FC values of in AMY/HPC_R (peak MNI coordinates= (24, -2, -20), blue circle in a) from the entire patient group,

treatment group, and HCs. The y-axis represents the mean FC values within the cluster, while the x-axis corresponds to different groups, the horizontal line represents the mean FC value for the group; right: mean BEN of AMY/HPC_R before and after treatment for the treatment cohort. The y-axis represents the mean FC values within the cluster, while the x-axis corresponds to the different treatment stages. b) left: mean baseline FC values of in AMY/HPC_L (peak MNI coordinates = (26, 0, -24), blue circle in b) from the entire patient group, treatment group, and HCs. The y-axis represents the mean FC values within the cluster, while the x-axis corresponds to the different groups, and the horizontal line represents the mean FC value for the group; right: mean BEN values of AMY/HPC_L before and after treatment for the treatment cohort. The y-axis represents the mean FC values within the cluster, while the x-axis corresponds to different treatment stages. c) left: mean baseline FC values of in HPC_L (peak MNI coordinates = (-28, -33, -7), blue circle in c) from the entire patient group, treatment group, and HCs. The y-axis represents the mean FC values within the cluster, while the x-axis corresponds to different groups, the horizontal line represents the mean FC value for the group; right: mean FC values of HPC_L before and after treatment for the treatment cohort. The y-axis represents the mean FC values within the cluster, while the x-axis corresponds to different treatment stages. The number under each slice indicates its location along the x-axis or y-axis in the MNI space, and L means left hemisphere, R means right hemisphere. * p<0.05, **p<0.01.

Correlation analysis indicated that higher BDI scores in the DEP group and Treat Pre group were positively related to higher FC of the left DLPFC- left AMY while higher SDS scores and RRS scores were negatively related to higher FC of the left DLPFC- right DLPFC (Table 6).

Table 6. Correlations of FC to clinical measures

Brain Region	Peak MNI Coordinate (X, Y, Z)	SDS		BDI		RRS	
		DEP	Treat Pre	DEP	Treat Pre	DEP	Treat Pre
AMY_R	(24, -2, -20)	0.097	0.113	0.258	0.409	0.163	0.314
AMY_L	(-26,0, -24)	0.003	0.371	0.346*	0.701**	-0.014	0.544
HPC_L	(-28, -33, -7)	-0.004	0.447	-0.014	0.422	0.059	0.009
DLPFC_R	(36, 51, 27)	-0.335*	0.100	-0.240	0.298	-0.382*	0.117

Note: SDS: Zung Self Rating Depression Scale, BDI: Beck Depression Inventory, RRS: Rumination Response Scale. L: left hemisphere, R: right hemisphere. * p<0.05, **p<0.01.

5 Discussion

This study evidenced that BEN alterations in depressed patients can be reverted through nonpharmacological treatment. Increased BEN in the left DLPFC, limbic system, and

precuneus in individuals with mild to moderate depression, compared to the HCs group, can be alleviated by nonpharmacological treatment at the individual level. Subsequent whole-brain FC analysis, utilizing the left DLPFC as the seed, revealed a substantial enhancement in FC with the right DLPFC, evident at both group and individual levels.

Increased BEN were mainly observed in the left DLPFC and limbic system (AMY, PHPC/HPC) in patients with mild to moderate depression compared to HCs. Neurosynth-based functional decoding suggests that these brain areas are primarily related to emotion regulation and reward processing. DLPFC and the limbic system are pivotal to top-down and bottom-up regulation. Increased BEN in these regions may be related to dysfunction of emotion regulation and reward systems, which are common symptoms in depression.

DLPFC, as a key component of the Executive Control Network (ECN, also known as the fronto-parietal network (FPN)), plays a central role in cognitive executive functions, working memory (Petrides 2000), cognitive flexibility (Kim, Johnson et al. 2011), and planning (Kaller, Rahm et al. 2011). It is also crucial for emotion regulation (Golkar, Lonsdorf et al. 2012, Hartling, Metz et al. 2021, Nejati, Majdi et al. 2021) and reward processing (Rushworth, Noonan et al. 2011, Overman, Sarrazin et al. 2023), probably through top-down regulation (Drevets and Raichle 1992, Simpson, Öngür et al. 2000). An increase in DLPFC activity has been shown to facilitate emotion regulation and improve cognitive control (Chen, Oei et al. 2023), and impaired emotional regulation due to DLPFC dysfunction is closely related to depression, in which the complex interaction between cognition and emotion is significantly disrupted (Salehinejad, Ghanavai et al. 2017). Previous studies have repeatedly shown a negative correlation between DLPFC and AMY (Davidson and Irwin 1999, Mayberg, Liotti et al. 1999, Damasio, Grabowski et al. 2000), demonstrating top-down control of emotion through increased DLPFC recruitment (Bishop 2008, Iordan, Dolcos et al. 2013) to down-regulate activity in AMY (Loos, Schicktanz et al. 2020, de Voogd and Hermans 2022). Impaired DLPFC regulation has been postulated to be a major mechanism of dys-emotional control, reflected in increased AMY activity, which may subsequently exacerbate the problem through bottom-up regulation (DeRubeis, Siegle et al. 2008). This assumption was supported by our FC analysis. Compared to HCs, depressed individuals showed opposite and much weaker FC between the left DLPFC and AMY (the FC was negative in HCs but became

slightly positive in patients). The FC magnitude reduction is contributed by the BEN increase in the left DLPFC. Increased BEN corresponds to lower coherence of brain activity, resulting in reduced correlation between left DLPFC and AMY. The FC direction change could be driven by the increased AMY activity, spreading into the left DLPFC via the bottom-up connection, leading to a positive FC between the two regions.

The limbic system is widely known for its involvement in reward, motivation, addiction, emotions, and memory. A substantial body of research has already demonstrated the crucial role of amygdala in emotion regulation (LeDoux 2003, Phelps and LeDoux 2005), and positioned it as a core component within the emotional brain network (LeDoux and Phelps 1993, Pessoa 2017) (Geissberger, Tik et al. 2020). Meanwhile, amygdala is also implicated in encoding reward functions (Baxter and Murray 2002, Murray 2007, Zhang, Kim et al. 2020). Hippocampus and parahippocampal cortex are known to be related to learning and memory, as well as episodic memory and emotion regulation. In the context of depression, meta-analyses and empirical studies have shown a reduction in the volume of AMY and PHPC/HPC in depressed patients (Sheline, Gado et al. 2003, Videbech and Ravnkilde 2004, Hamilton, Siemer et al. 2008, Sacher, Neumann et al. 2012, Redlich, Opel et al. 2018). Based on task fMRI data, patients with depression showed relatively more AMY activity when viewing emotional faces than HCs, particularly on the left side (Peluso, Glahn et al. 2009, Yang, Simmons et al. 2010), and sustained AMY activity is associated with increased and sustained emotional reactivity in MDD (Siegle, Thompson et al. 2007). Through the projections from AMY to PHPC/HPC, which subserves the creation and maintenance of emotional associations in memory, increased processing of negative emotion in AMY (Disner, Beevers et al. 2011) may ultimately lead to a persistent negative associations (Sheline, Sanghavi et al. 1999, DeRubeis, Siegle et al. 2008, Dolcos, Iordan et al. 2011).

In this study, we found that nonpharmacological treatment reversed the BEN increase in the left DLPFC and limbic system in depressed individuals. These treatment effects were generally consistent with what we found before (Liu, Song et al. 2019, Liu, Song et al. 2020) where higher MOFC/sgACC BEN was associated with higher depression severity in MDD, and an 8-week successful antidepressant treatment in MDD showed a reduction of BEN in MOFC/sgACC and HPC. DLPFC and the limbic system are closely linked to emotion

regulation and depression (Zelazo and Cunningham 2007, Warren, Heller et al. 2021).Reversing the altered BEN patterns in these regions in depression may facilitate the restoration of dysregulated top-down emotion regulation abilities. Through a seed-based FC analysis using the left DLPFC cluster identified in the longitudinal BEN comparison, we found increased FC between left DLPFC and right DLPFC and decreased FC between the left DLPFC and left AMY after nonpharmacological treatment. Consistent with the cross-sectional and longitudinal BEN analysis results, the FC results also clearly showed that nonpharmacological treatment reversed the impaired FC in depressed individuals. These reversals may indicate an improvement in executive control function and increased inhibition function for the limbic system.

We also found decreased BEN in SMG, IPL, IFG, PCu, and LHb after treatment. Like DLPFC, the SMG and IPL are parts of the ECN, and the observed BEN reduction in these regions after treatment further suggests an improvement in executive control. The IFG is implicated in emotion regulation (Goldin, McRae et al. 2008, Morawetz, Bode et al. 2017), and the decreased BEN within the IFG after treatment may indicate an improvement in emotion regulation. PCu showed increased BEN in depressed patients compared to HCs. Consistent with DLPFC and AMY, the PCu BEN increase was reversed after treatment. PCu is a functional core of the DMN (Utevsky, Smith et al. 2014) and is involved in processing internal mental states (Menon 2023). Increased PCu BEN may reflect a reduced internal mental state processing, which can be partially supported by the reproducible increase in PCu during rumination (Song, et al. 2023). Increased BEN in LHb could reflect the altered brain functions such as reward behavior, aversive behavior, and behavioral flexibility subserved by habenula (Hu, Cui et al. 2020). SMN (PSC and PMC) and temporal cortex (MTG, ITG, and pSTS) are also implicated in depression (Takahashi, Yücel et al. 2010, Ray, Bezmaternykh et al. 2021). Our previous study showed aberrant BEN in these regions (Liu, Song et al. 2019). Accordingly, BEN reductions in the SMN and temporal cortex after treatment may indicate improvement in depression.

6 Conclusion

Patients with mild to moderate depression had increased BEN in the left DLPFC and lim bic system, which was suppressed or reversed by nonpharmacological treatment. BEN in the DLPFC and limbic system could be a potential personalized marker for assessing depression and the effectiveness of nonpharmacological treatments.

Data and code availability

The raw data is available from OpenNeuro coded as ds002748 (https://openneuro.org/datasets/ds002748) and ds003007 (https://openneuro.org/datasets/ds003007).

All unthreholded statistical maps are available at https://neurovault.org/collections/YSQTCFYO/ or https://github.com/donghui1119/Brain_Entropy_Project/tree/main/Depression/Nonpharmacological_Treatment (upon publication of the manuscript).

BENtbx is available from https://www.cfn.upenn.edu/zewang/BENtbx.php.

Customed python scripts and further updates related to the study will be available at https://github.com/donghui1119/Brain_Entropy_Project/tree/main/Depression/Nonpharmacological_Treatment (upon publication of the manuscript).

Acknowledgements

We thank Dmitry D Bezmaternykh et al for releasing their dataset. Yin Wang was supported by Open Research Fund of the State Key Laboratory of Cognitive Neuroscience and Learning (CNLZD2103), National Science and Technology Innovation 2030 Major Program (2022ZD0211000), and Fundamental Research Funds for the Central Universities (2233300002).

CRediT authorship contribution statement

Dong-Hui Song: conceptualization, data curation, data analysis, visualization, manuscript drafting and editing. Yin Wang: manuscript editing, supervision, project administration, acquisition of funding. Ze Wang: conceptualization, manuscript editing and final manuscript proofing, supervision, project administration.

References :

Baxter, M. G. and E. A. Murray (2002). "The amygdala and reward." Nature reviews neuroscience **3**(7): 563-573.

Beck, A. T., R. A. Steer and G. K. Brown (1987). Beck depression inventory, Harcourt Brace Jovanovich New York:.

Bezmaternykh, D. D., M. Y. Melnikov, A. A. Savelov, L. I. Kozlova, E. D. Petrovskiy, K. A. Natarova and M. B. Shtark (2021). "Brain networks connectivity in mild to moderate depression: Resting state fmri study with implications to nonpharmacological treatment." Neural Plasticity **2021**.

Bishop, S. J. (2008). "Neural mechanisms underlying selective attention to threat." Annals of the New York Academy of Sciences **1129**(1): 141-152.

Camargo, A., G. Del Mauro and Z. Wang (2024). "Task-induced changes in brain entropy." Journal of Neuroscience Research **102**(2): e25310.

Chang, D., D. Song, J. Zhang, Y. Shang, Q. Ge and Z. Wang (2018). "Caffeine caused a widespread increase of resting brain entropy." Scientific reports **8**(1): 2700.

Chaudhury, D., H. Liu and M.-H. Han (2015). "Neuronal correlates of depression." Cellular and Molecular Life Sciences **72**: 4825-4848.

Chen, L., T. P. Oei and R. Zhou (2023). "The cognitive control mechanism of improving emotion regulation: A high-definition tDCS and ERP study." Journal of Affective Disorders **332**: 19-28.

Clausius, R. J. E. (1862). Ueber die wärmeleitung gasförmiger körper, Verlag nicht ermittelbar.

Damasio, A. R., T. J. Grabowski, A. Bechara, H. Damasio, L. L. Ponto, J. Parvizi and R. D. Hichwa (2000). "Subcortical and cortical brain activity during the feeling of self-generated emotions." Nature

neuroscience **3**(10): 1049-1056.

Davidson, R. J. and W. Irwin (1999). "The functional neuroanatomy of emotion and affective style." Trends in cognitive sciences **3**(1): 11-21.

De Ridder, D., S. Vanneste and W. Freeman (2014). "The Bayesian brain: phantom percepts resolve sensory uncertainty." Neuroscience & Biobehavioral Reviews **44**: 4-15.

de Voogd, L. D. and E. J. Hermans (2022). "Meta-analytic evidence for downregulation of the amygdala during working memory maintenance." Human Brain Mapping **43**(9): 2951-2971.

Del Mauro, G. and Z. Wang (2023). "Associations of brain entropy estimated by resting state fMRI with physiological indices, body mass index, and cognition." Journal of Magnetic Resonance Imaging.

DeRubeis, R. J., G. J. Siegle and S. D. Hollon (2008). "Cognitive therapy versus medication for depression: treatment outcomes and neural mechanisms." Nature Reviews Neuroscience **9**(10): 788-796.

Disner, S. G., C. G. Beevers, E. A. Haigh and A. T. Beck (2011). "Neural mechanisms of the cognitive model of depression." Nature Reviews Neuroscience **12**(8): 467-477.

Dolcos, F., A. D. Iordan and S. Dolcos (2011). "Neural correlates of emotion–cognition interactions: A review of evidence from brain imaging investigations." Journal of Cognitive Psychology **23**(6): 669-694.

Donghui Song, W., J. Zhang, Y. Shang and Z. Wang (2017). Decreased brain entropy by 20 Hz rTMS on the left dorsolateral prefrontal cortex. Annual meeting of International Congress of MRI, Seoul, Korea.[Google Scholar].

Drevets, W. C. and M. E. Raichle (1992). "Neuroanatomical circuits in depression: implications for treatment mechanisms." Psychopharmacology bulletin **28**(3): 261-274.

Friston, K., J. Kilner and L. Harrison (2006). "A free energy principle for the brain." Journal of physiology-Paris **100**(1-3): 70-87.

Fu, S., S. Liang, C. Lin, Y. Wu, S. Xie, M. Li, Q. Lei, J. Li, K. Yu and Y. Yin (2023). "Aberrant brain entropy in posttraumatic stress disorder comorbid with major depressive disorder during the coronavirus disease 2019 pandemic." Frontiers in Psychiatry **14**: 1143780.

Geissberger, N., M. Tik, R. Sladky, M. Woletz, A.-L. Schuler, D. Willinger and C. Windischberger (2020). "Reproducibility of amygdala activation in facial emotion processing at 7T." NeuroImage **211**: 116585.

Goldin, P. R., K. McRae, W. Ramel and J. J. Gross (2008). "The neural bases of emotion regulation: reappraisal and suppression of negative emotion." Biological psychiatry **63**(6): 577-586.

Golkar, A., T. B. Lonsdorf, A. Olsson, K. M. Lindstrom, J. Berrebi, P. Fransson, M. Schalling, M. Ingvar and A. Öhman (2012). "Distinct contributions of the dorsolateral prefrontal and orbitofrontal cortex during emotion regulation." PloS one **7**(11): e48107.

Gorgolewski, K., C. D. Burns, C. Madison, D. Clark, Y. O. Halchenko, M. L. Waskom and S. S. Ghosh (2011). "Nipype: a flexible, lightweight and extensible neuroimaging data processing framework in python." Frontiers in neuroinformatics **5**: 13.

Gorgolewski, K. J., G. Varoquaux, G. Rivera, Y. Schwarz, S. S. Ghosh, C. Maumet, V. V. Sochat, T. E. Nichols, R. A. Poldrack and J.-B. Poline (2015). "NeuroVault. org: a web-based repository for collecting and sharing unthresholded statistical maps of the human brain." Frontiers in neuroinformatics **9**: 8.

Greve, D. N. and B. Fischl (2009). "Accurate and robust brain image alignment using boundary-based registration." Neuroimage **48**(1): 63-72.

Hamilton, J. P., M. Siemer and I. H. Gotlib (2008). "Amygdala volume in major depressive disorder: a meta-analysis of magnetic resonance imaging studies." Molecular psychiatry **13**(11): 993-1000.

Hartling, C., S. Metz, C. Pehrs, M. Scheidegger, R. Gruzman, C. Keicher, A. Wunder, A. Weigand and S. Grimm (2021). "Comparison of four fMRI paradigms probing emotion processing." Brain Sciences **11**(5): 525.

Hu, H., Y. Cui and Y. Yang (2020). "Circuits and functions of the lateral habenula in health and in disease." Nature Reviews Neuroscience **21**(5): 277-295.

Hudson, J. I., B. Mangweth, H. G. Pope, C. De Col, A. Hausmann, S. Gutweniger, N. M. Laird, W. Biebl and M. T. Tsuang (2003). "Family study of affective spectrum disorder." Archives of General Psychiatry **60**(2): 170-177.

Iordan, A. D., S. Dolcos and F. Dolcos (2013). "Neural signatures of the response to emotional distraction: a review of evidence from brain imaging investigations." Frontiers in human neuroscience **7**: 200.

Jenkinson, M., P. Bannister, M. Brady and S. Smith (2002). "Improved optimization for the robust and accurate linear registration and motion correction of brain images." Neuroimage **17**(2): 825-841.

Jenkinson, M. and S. Smith (2001). "A global optimisation method for robust affine registration of brain images." Medical image analysis **5**(2): 143-156.

Ji, S., Y. Zhang, N. Chen, X. Liu, Y. Li, X. Shao, Z. Yang, Z. Yao and B. Hu (2022). "Shared increased entropy of brain signals across patients with different mental illnesses: A coordinate-based activation likelihood estimation meta-analysis." Brain Imaging and Behavior: 1-8.

Jiang, W., L. Cai and Z. Wang (2023). "Common hyper-entropy patterns identified in nicotine smoking, marijuana use, and alcohol use based on uni-drug dependence cohorts." Medical & Biological

Engineering & Computing: 1-8.

Kaller, C. P., B. Rahm, J. Spreer, C. Weiller and J. M. Unterrainer (2011). "Dissociable contributions of left and right dorsolateral prefrontal cortex in planning." Cerebral cortex **21**(2): 307-317.

Kim, C., N. F. Johnson, S. E. Cilles and B. T. Gold (2011). "Common and distinct mechanisms of cognitive flexibility in prefrontal cortex." Journal of Neuroscience **31**(13): 4771-4779.

Klooster, D. C. and S. H. Siddiqi (2023). "Embracing the heterogeneity in depression neuroimaging." Nature Mental Health **1**(4): 243-244.

Kuang, L., W. Gao, L. Wang, Y. Guo, W. Cao, D. Cui, Q. Jiao, J. Qiu, L. Su and G. Lu (2021). "Increased resting-state brain entropy of parahippocampal gyrus and dorsolateral prefrontal cortex in manic and euthymic adolescent bipolar disorder." Journal of Psychiatric Research **143**: 106-112.

LeDoux, J. (2003). "The emotional brain, fear, and the amygdala." Cellular and molecular neurobiology **23**: 727-738.

LeDoux, J. E. and E. A. Phelps (1993). "Emotional networks in the brain." Handbook of emotions **109**: 118.

Li, Z., Z. Fang, N. Hager, H. Rao and Z. Wang (2016). "Hyper-resting brain entropy within chronic smokers and its moderation by Sex." Scientific reports **6**(1): 29435.

Lin, C., S.-H. Lee, C.-M. Huang, G.-Y. Chen, P.-S. Ho, H.-L. Liu, Y.-L. Chen, T. M.-C. Lee and S.-C. Wu (2019). "Increased brain entropy of resting-state fMRI mediates the relationship between depression severity and mental health-related quality of life in late-life depressed elderly." Journal of affective disorders **250**: 270-277.

Lin, L., D. Chang, D. Song, Y. Li and Z. Wang (2022). "Lower resting brain entropy is associated with stronger task activation and deactivation." NeuroImage **249**: 118875.

Liu, X., D. Song, Y. Yin, C. Xie, H. Zhang, H. Zhang, Z. Zhang, Z. Wang and Y. Yuan (2019). The role of brain entropy on antidepressant effect in major depressive disorder. PSYCHOTHERAPY AND PSYCHOSOMATICS, KARGER ALLSCHWILERSTRASSE 10, CH-4009 BASEL, SWITZERLAND.

Liu, X., D. Song, Y. Yin, C. Xie, H. Zhang, H. Zhang, Z. Zhang, Z. Wang and Y. Yuan (2020). "Altered Brain Entropy as a predictor of antidepressant response in major depressive disorder." Journal of Affective Disorders **260**: 716-721.

Loos, E., N. Schicktanz, M. Fastenrath, D. Coynel, A. Milnik, B. Fehlmann, T. Egli, M. Ehrler, A. Papassotiropoulos and D. J.-F. de Quervain (2020). "Reducing amygdala activity and phobic fear through cognitive top–down regulation." Journal of Cognitive Neuroscience **32**(6): 1117-1129.

Magistretti, P. J. and I. Allaman (2015). "A cellular perspective on brain energy metabolism and functional imaging." Neuron **86**(4): 883-901.

Mayberg, H. S., M. Liotti, S. K. Brannan, S. McGinnis, R. K. Mahurin, P. A. Jerabek, J. A. Silva, J. L. Tekell, C. C. Martin and J. L. Lancaster (1999). "Reciprocal limbic-cortical function and negative mood: converging PET findings in depression and normal sadness." American journal of psychiatry **156**(5): 675-682.

Menon, V. (2023). "20 years of the default mode network: A review and synthesis." Neuron.

Morawetz, C., S. Bode, J. Baudewig and H. R. Heekeren (2017). "Effective amygdala-prefrontal connectivity predicts individual differences in successful emotion regulation." Social cognitive and affective neuroscience **12**(4): 569-585.

Murray, E. A. (2007). "The amygdala, reward and emotion." Trends in cognitive sciences **11**(11): 489-497.

Nejati, V., R. Majdi, M. A. Salehinejad and M. A. Nitsche (2021). "The role of dorsolateral and

ventromedial prefrontal cortex in the processing of emotional dimensions." Scientific reports **11**(1): 1971.

Odum, H. T. (1988). "Self-organization, transformity, and information." Science **242**(4882): 1132-1139.

Overman, M. J., V. Sarrazin, M. Browning and J. O'Shea (2023). "Stimulating human prefrontal cortex increases reward learning." NeuroImage **271**: 120029.

Peluso, M. A., D. C. Glahn, K. Matsuo, E. S. Monkul, P. Najt, F. Zamarripa, J. Li, J. L. Lancaster, P. T. Fox and J.-H. Gao (2009). "Amygdala hyperactivation in untreated depressed individuals." Psychiatry Research: Neuroimaging **173**(2): 158-161.

Pessoa, L. (2017). "A network model of the emotional brain." Trends in cognitive sciences **21**(5): 357-371.

Petrides, M. (2000). "The role of the mid-dorsolateral prefrontal cortex in working memory." Experimental brain research **133**: 44-54.

Phelps, E. A. and J. E. LeDoux (2005). "Contributions of the amygdala to emotion processing: from animal models to human behavior." Neuron **48**(2): 175-187.

Power, J. D., K. A. Barnes, A. Z. Snyder, B. L. Schlaggar and S. E. Petersen (2012). "Spurious but systematic correlations in functional connectivity MRI networks arise from subject motion." Neuroimage **59**(3): 2142-2154.

Ray, D., D. Bezmaternykh, M. Mel'nikov, K. J. Friston and M. Das (2021). "Altered effective connectivity in sensorimotor cortices is a signature of severity and clinical course in depression." Proceedings of the National Academy of Sciences **118**(40): e2105730118.

Redlich, R., N. Opel, C. Bürger, K. Dohm, D. Grotegerd, K. Förster, D. Zaremba, S. Meinert, J. Repple and V. Enneking (2018). "The limbic system in youth depression: brain structural and functional

alterations in adolescent in-patients with severe depression." Neuropsychopharmacology **43**(3): 546-554.

Richman, J. S. and J. R. Moorman (2000). "Physiological time-series analysis using approximate entropy and sample entropy." American journal of physiology-heart and circulatory physiology **278**(6): H2039-H2049.

Rushworth, M. F., M. P. Noonan, E. D. Boorman, M. E. Walton and T. E. Behrens (2011). "Frontal cortex and reward-guided learning and decision-making." Neuron **70**(6): 1054-1069.

Sacher, J., J. Neumann, T. Fünfstück, A. Soliman, A. Villringer and M. L. Schroeter (2012). "Mapping the depressed brain: a meta-analysis of structural and functional alterations in major depressive disorder." Journal of affective disorders **140**(2): 142-148.

Salehinejad, M. A., E. Ghanavai, R. Rostami and V. Nejati (2017). "Cognitive control dysfunction in emotion dysregulation and psychopathology of major depression (MD): Evidence from transcranial brain stimulation of the dorsolateral prefrontal cortex (DLPFC)." Journal of affective disorders **210**: 241-248.

Schmaal, L., E. Pozzi, T. C. Ho, L. S. Van Velzen, I. M. Veer, N. Opel, E. J. Van Someren, L. K. Han, L. Aftanas and A. Aleman (2020). "ENIGMA MDD: seven years of global neuroimaging studies of major depression through worldwide data sharing." Translational psychiatry **10**(1): 172.

Shannon, C. E. (1948). "A mathematical theory of communication." The Bell system technical journal **27**(3): 379-423.

Sheline, Y. I., M. H. Gado and H. C. Kraemer (2003). "Untreated depression and hippocampal volume loss." American journal of psychiatry **160**(8): 1516-1518.

Sheline, Y. I., M. Sanghavi, M. A. Mintun and M. H. Gado (1999). "Depression duration but not age

predicts hippocampal volume loss in medically healthy women with recurrent major depression." Journal of Neuroscience **19**(12): 5034-5043.

Siegle, G. J., W. Thompson, C. S. Carter, S. R. Steinhauer and M. E. Thase (2007). "Increased amygdala and decreased dorsolateral prefrontal BOLD responses in unipolar depression: related and independent features." Biological psychiatry **61**(2): 198-209.

Simpson, J. R., D. Öngür, E. Akbudak, T. E. Conturo, J. M. Ollinger, A. Z. Snyder, D. A. Gusnard and M. E. Raichle (2000). "The emotional modulation of cognitive processing: an fMRI study." Journal of Cognitive Neuroscience **12**(Supplement 2): 157-170.

Smith, S. M., M. Jenkinson, M. W. Woolrich, C. F. Beckmann, T. E. Behrens, H. Johansen-Berg, P. R. Bannister, M. De Luca, I. Drobnjak and D. E. Flitney (2004). "Advances in functional and structural MR image analysis and implementation as FSL." Neuroimage **23**: S208-S219.

Sneyd, J., G. Theraula, E. Bonabeau, J.-L. Deneubourg and N. R. Franks (2001). Self-organization in biological systems, Princeton university press.

Sokunbi, M. O., W. Fung, V. Sawlani, S. Choppin, D. E. Linden and J. Thome (2013). "Resting state fMRI entropy probes complexity of brain activity in adults with ADHD." Psychiatry Research: Neuroimaging **214**(3): 341-348.

Song, D., D. Chang, J. Zhang, Q. Ge, Y.-F. Zang and Z. Wang (2019). "Associations of brain entropy (BEN) to cerebral blood flow and fractional amplitude of low-frequency fluctuations in the resting brain." Brain imaging and behavior **13**: 1486-1495.

Song, D., D. Chang, J. Zhang, W. Peng, Y. Shang, X. Gao and Z. Wang (2019). "Reduced brain entropy by repetitive transcranial magnetic stimulation on the left dorsolateral prefrontal cortex in healthy young adults." Brain imaging and behavior **13**: 421-429.

Song, D., J. Z. Da Chang, Q. Ge, Y.-F. Zang and Z. Wang (2018). "Associations between Resting Brain Entropy (BEN) and Fractional Amplitude of low-frequency fluctuation (fALFF)."

Spasojević, J. and L. B. Alloy (2001). "Rumination as a common mechanism relating depressive risk factors to depression." Emotion **1**(1): 25.

Takahashi, T., M. Yücel, V. Lorenzetti, M. Walterfang, Y. Kawasaki, S. Whittle, M. Suzuki, C. Pantelis and N. B. Allen (2010). "An MRI study of the superior temporal subregions in patients with current and past major depression." Progress in Neuro-Psychopharmacology and Biological Psychiatry **34**(1): 98-103.

Utevsky, A. V., D. V. Smith and S. A. Huettel (2014). "Precuneus is a functional core of the default-mode network." Journal of Neuroscience **34**(3): 932-940.

Videbech, P. and B. Ravnkilde (2004). "Hippocampal volume and depression: a meta-analysis of MRI studies." American Journal of Psychiatry **161**(11): 1957-1966.

Wang, Z. (2021). "The neurocognitive correlates of brain entropy estimated by resting state fMRI." NeuroImage **232**: 117893.

Wang, Z. (2021). "Resting state fMRI-based temporal coherence mapping." arXiv preprint arXiv:2109.00146.

Wang, Z. and A. s. D. N. Initiative (2020). "Brain entropy mapping in healthy aging and Alzheimer's disease." Frontiers in Aging Neuroscience **12**: 596122.

Wang, Z., Y. Li, A. R. Childress and J. A. Detre (2014). "Brain entropy mapping using fMRI." PloS one **9**(3): e89948.

Warren, S. L., W. Heller and G. A. Miller (2021). "The structure of executive dysfunction in depression and anxiety." Journal of Affective Disorders **279**: 208-216.

Whisman, M. A., A. du Pont and P. Butterworth (2020). "Longitudinal associations between rumination and depressive symptoms in a probability sample of adults." Journal of Affective Disorders **260**: 680-686.

Xue, S.-W., Q. Yu, Y. Guo, D. Song and Z. Wang (2019). "Resting-state brain entropy in schizophrenia." Comprehensive Psychiatry **89**: 16-21.

Yan, C.-G., X. Chen, L. Li, F. X. Castellanos, T.-J. Bai, Q.-J. Bo, J. Cao, G.-M. Chen, N.-X. Chen and W. Chen (2019). "Reduced default mode network functional connectivity in patients with recurrent major depressive disorder." Proceedings of the National Academy of Sciences **116**(18): 9078-9083.

Yang, T. T., A. N. Simmons, S. C. Matthews, S. F. Tapert, G. K. Frank, J. E. Max, A. Bischoff-Grethe, A. E. Lansing, G. Brown and I. A. Strigo (2010). "Adolescents with major depression demonstrate increased amygdala activation." Journal of the American Academy of Child & Adolescent Psychiatry **49**(1): 42-51.

Yarkoni, T., R. A. Poldrack, T. E. Nichols, D. C. Van Essen and T. D. Wager (2011). "Large-scale automated synthesis of human functional neuroimaging data." Nature methods **8**(8): 665-670.

Zelazo, P. D. and W. A. Cunningham (2007). "Executive function: Mechanisms underlying emotion regulation."

Zhang, X., J. Kim and S. Tonegawa (2020). "Amygdala reward neurons form and store fear extinction memory." Neuron **105**(6): 1077-1093. e1077.

Zhang, Y., M. Brady and S. Smith (2001). "Segmentation of brain MR images through a hidden Markov random field model and the expectation-maximization algorithm." IEEE transactions on medical imaging **20**(1): 45-57.

Zhou, F., R. Xu, E. Dowd, Y. Zang, H. Gong and Z. Wang (2014). "Alterations in regional functional

coherence within the sensory-motor network in amyotrophic lateral sclerosis." Neuroscience letters **558**: 192-196.

Zhou, F., Y. Zhuang, H. Gong, J. Zhan, M. Grossman and Z. Wang (2016). "Resting State Brain Entropy Alterations in Relapsing Remitting Multiple Sclerosis." PLoS One **11**(1): e0146080.

Zung, W. W. (1965). "A self-rating depression scale." Archives of general psychiatry **12**(1): 63-70.